3D-printed Optical Devices with Refractive Index Control for Microwave Applications

D. Isakov[1], 2, Y. Wu[2], B. Allen[3], C. J. Stevens[3] and P. S. Grant[2]

[1] WMG, University of Warwick, Coventry CV4 7AL, United Kingdom, d.isakov@warwick.ac.uk
[2] Department of Materials, University of Oxford, Oxford OX1 3PH, United Kingdom
[3] Department of Materials, University of Oxford, Oxford OX1 3PH, United Kingdom

ABSTRACT

We present the design, simulation, fused deposition modelling (FDM) 3D printing and characterisation of several structures with spatial variations in refractive index. The 3D-printed structures represent optical devices such as a gradient refractive index (GRIN) lens, a quarter-wave plate, band-absorbers and a GRIN spiral phase plate, all designed to operate in the 12–18 GHz frequency range. The devices were fabricated by using two printheads and bespoke filaments with 'high' and 'low' dielectric permittivity to provide high contrast (up to $\Delta n = 2$) in refractive index thus allowing structures with reduced size. The manufactured devices showed a good agreement with simulation and theoretically predicted performance.

Keywords: RF, gradient index, phase plate, 3D printing

1 Introduction

Achieving sub-wavelength spatial variations in the relative permittivity ϵ_r and permeability μ_r to control the propagation of the electromagnetic radiation opens up many opportunities for the development of new devices with improved or novel functionality [1]. However, while the progress in Transformational Optics (TO) theory continues to suggest many beneficial designs and functions, the application of this principle in practice has remained complicated due to the difficulty of fabricating structures with the required controlled spatial distribution of permittivity and/or permeability.

Recent rapid development of additive manufacturing and related 3D printing techniques have shown how these approaches might reduce the production time and simplify the manufacturing process of materials and devices with the required control of the spatial distribution of the demanded properties [2, 3, 4]. 3D printing offers a flexible and scalable capability for the fabrication of objects with a complex form factor [5, 6] and may provide a significant contrast in the spatial variation of refractive index [7]. Recently, the ability to fabricate new FDM feedstock filament materials with high dielectric permittivity up to $\epsilon_r = 11$ suitable for mass-market 3D printing has been demonstrated [8]. Utilising such filament would allow rapid prototyping of devices for RF and microwave applications where high contrast in the index of refraction n is required and may open new possibilities for implementation of principles of TO in practice. Another benefit of high-ϵ filament is that devices can be fabricated with reduced size (along the direction of propagation) without a change in overall optical path nl and device performance [7].

In this paper, we summarise our recent progress in design, fabrication, and characterisation of several electromagnetic devices able to manipulate the propagated wave through a spatially graded refractive index. Four all-dielectric devices such as a metamaterial tunable absorber, a GRIN lens, a spiral phase plate and a quarter-wave phase plate were 3D printed using fused deposition modelling and our bespoke feedstock composite filaments with dielectric permittivity in the range 7 to 11. Although these optical elements were designed mainly to operate at single frequency 15 GHz, they show good capability in the broad frequency range in 12–18 GHz.

2 Results

2.1 Metamaterial absorber and anisotropic phase plate

A simple 3D-printed all-dielectric metamaterial absorber, as described in [9], consists of arrays of alternating low permittivity (ABS plastic) and high permittivity (ceramic composite) stripes with thickness much lower than the wavelength aligned along the H-field of the propagating wave. For investigation of any metamaterial features, the printed striped sample was placed in a Ku-band waveguide flange, as shown in Figure 1(a). The alternating dielectric stripes present a periodic array of rectangular-shaped dielectric resonators and can produce a Mie-type magnetic resonance induced by a large displacement current in dielectric stripes with high permittivity, and can be attributed to the creation of an artificial magnetic dipole [10].

Figure 1(b) shows measured transmittance $T = |S_{21}|^2$, reflectance $R = |S_{11}|^2$, and absorption $A = 1 - R - T$ obtained from a 3D-printed sample containing 2 high permittivity stripes with $\epsilon_2 = 11 + i0.078$ interleaved

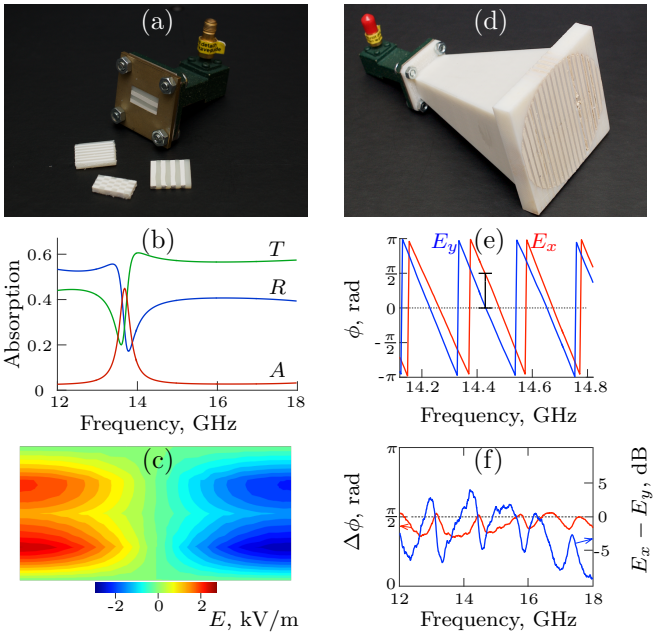

Figure 1: (a) Photograph of the 3D-printed dielectric coupon $16 \times 8 \times 2$ mm^3 with alternating stripes with $\epsilon_1 = 2.56 \cdot (1 + i0.002)$ and $\epsilon_2 = 11 \cdot (1 + i0.007)$; (b) the transmission T, reflection R and absorption A parameters measured in the coupon made of 4-stripes; (c) electric field distribution in the coupon at the resonance. (d) Photograph of the 3D-printed piramidal horn antenna and a quarter-wave plate; (e) the phases ϕ of the recieved y and x components of the electrtic field; (f) the phase difference $\Delta\phi$ between x and y components of the polarization in the P-QWP45-S arrangement showing that the linear polarisation of the incident wave is transformed into circular (elliptical) polarisation in the 12–18 GHz frequency range.

between low permittivity stripes with $\epsilon_1 = 2.56 + i0.005$. An absorption of 50% was obtained near 1.38 GHz. Figure 1(c) shows simulated distributions of the transverse electric field inside the sample at the resonant frequency. The circular component of electric field, shown as concentric curves in the z-plane, resulted in a strong magnetic field and was associated with the first TE_{11} mode of the Mie resonance.

According to effective medium theory [11], a periodic two-component structure with alternating permittivity ϵ_1 and ϵ_2 will have an anisotropy in effective relative dielectric permittivity ϵ_{eff} with values between low and high Wiener bounds: $\epsilon_{min}^{-1} = f\epsilon_2^{-1} + (1-f)\epsilon_1^{-1}$ and $\epsilon_{max} = f\epsilon_2 + (1-f)\epsilon_1$, where f is the volume fill fraction of the high permittivity component. This opens up the possibility for design the anisotropic structures with controlled birefringence to transform or control the mode of polarization in electromagnetic waves. One of the examples of such device is a quarter-wave and/or half-wave plate. Figure 1(d) presents a 3D-printed quarter-wave plate (QWP) designed in such a way that an optical path difference Δl between vertical and horizontal components of the plane wave will result in phase delay $\delta = \pm\pi/2$. Figure 1(e) shows the experimental results for the phase of the linearly polarised wave (vertical P-polarization) passing through the QWP oriented at 45° to their principal axes to the polarisation of incident beam (P) and analysed by the receiver antenna with either vertical polarisation (E_x component) or linear horizontal S polarisation (E_y component). Figure 1(f) presents the phase (red) and amplitude (blue) difference between orthogonal components of the electric field. These results show that original linearly polarised wave (with only E_x component) has been transformed by the QWP to the circularly (elliptically) polarised wave with nearly equal E_x and E_y amplitudes and a phase difference of approximately $\pi/2$.

2.2 Gradient index devices

Gradient index devices present an alternative ways to manipulate and control an electromagnetic wave, which passing through a boundary between two homogeneous media will experience a phase delay proportional to the difference in refractive index of the media. Thus in GRIN devices, the beam manipulation mechanism is based on the phase shift of the electromagnetic wave resulting from its interaction with a medium with a spatially graded refractive index.

Figure 2(a) shows 3D-printed H-plane sectoral horn with relatively small length $R_0 = 2\lambda$ and a 3D-printed flat GRIN lens over the horn aperture to produce improved directivity. The desired functionality of the GRIN lens was achieved through the appropriate distribution of the refractive index using a ray tracing principle of the compensation of the ray phase retardation $\delta = \frac{2\pi}{\lambda} Ln$, where λ is a wavelength, and Ln is an optical pathway of the ray [7]. Figure 2(b) shows 2D simulations of the far-field radiation pattern for the shortened horn and discretised GRIN lens in a predicting excellent directivity at 15 GHz. The experimental results (Figure 2(c)) are in good agreement with simulation. The horn with length only 2λ coupled with 3D-printed GRIN lens has the same directivity of approximately 18 dBi as a high-directivity horn with optimal length 6λ. Overall, when the GRIN lens is combined with an open aperture horn with a reduced length of 2λ, improved antenna directivity is achieved while simultaneously reducing the overall antenna physical length by over a factor of three.

Besides GRIN lens, TO approaches with a spatially varying refractive index can be utilised to design many other devices, such as cloaks, photonics crystals, power dividers [13] or a spiral phase plate (SPP). The later one is able to manipulate the plane wave into a helically phased beam with orbital angular momentum (OAM) [12]. Such phase plates are very promising for

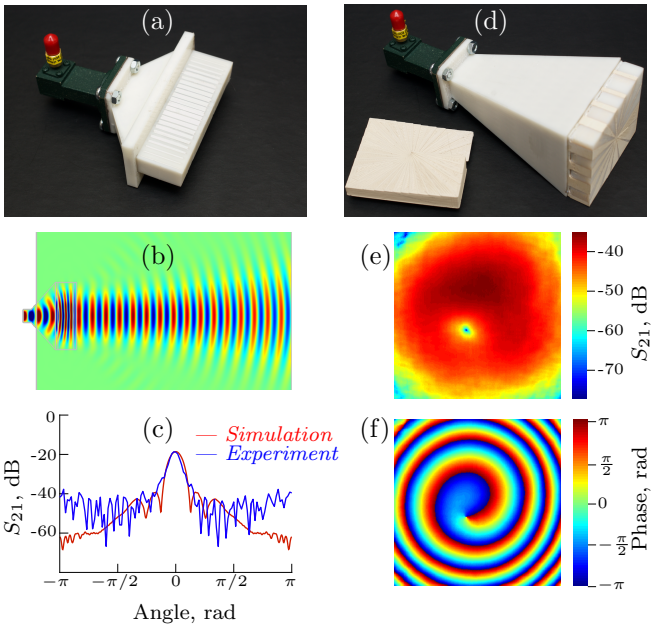

Figure 2: (a) Photograph of the 3D-printed H-plane short (2λ) horn with 3D-printed GRIN lens attached at the front aperture; (b) simulated electric field distribution in the horn-lens arrangements; (c) experimental and simulated far-field radiation patterns of the short horn with 3D-printed GRIN lens. (d) Photograph of the 3D-printed horn antenna with GRIN spiral phase plate (the plate with azimuthal dependent thickness is also shown); (e) and (f) experimental measurements of the 15 GHz radiation signal from the GRIN spiral phase plate in the plane with area 70×70 cm^2 perpendicular to the propagation vector.

applications required high data transfer rates. This is possible due to the multiplexing of parallel data streams through several independent orbital angular momentum modes.

In general, a spiral phase plate is a dielectric material with an azimuthally dependent height (usually in discrete height steps) that imparts an azimuthal phase shift onto incident radiation resulting in OAM. The total step height is that the total phase shift around the centre of the plate is $\pm m2\pi$, where m is an integer denoting the mode of the OAM. Alternatively, a GRIN spiral phase plate can be obtained when the azimuthal phase shift is instead induced through the azimuthally varied refractive index. Both such plates (with azimuthally varying height and refractive index) have been 3D-printed and are shown in Figure 2(d).

Figures 2(e) and 2(f) present the experimental results of the amplitude and phase profiles of the z-plane perpendicular to the direction of propagation, obtained from a 3D-printed GRIN spiral phase plate, measured with a millimetre step resolution scanning system at the distance about 50λ from the SPP. The amplitude pattern in Figure 2(e) exhibits the expected vortex with a null intensity in the centre, whereas the spatial phase profile in Figure 2(f) exhibits the phase profile related to an OAM $m = -1$. It should be noted that although the GRIN SPP was designed to operate at single frequency 15 GHz, it remains a good capability in the 12–18 GHz frequency range.

3 Conclusion

Our recent achievements in formulation and fabrication of feedstock filaments with high dielectric permittivity for FDM 3D printing allows convenient implementation of the principles of transformation electromagnetics for the design and fabrication of several types of optical devices to be operated in the microwave frequency band. Despite their relative simplicity, the experimental realisation of these graded refractive index devices shows that there is a significant opportunity for 3D printing to enable TO-inspired devices in the microwave domain, especially as higher dielectric constant materials suitable for 3D printing become available.

Acknowledgment

This work was funded by the UK Engineering and Physical Sciences Research Council (EP/I034548/1 and EP/P005578/1). BA is grateful to the support of the Royal Society Industry fellowship scheme under award number IF160001.

REFERENCES

[1] J. B. Pendry, D. Schurig and D. R. Smith, *Controlling electromagnetic fields*, Science, 312, 1780–1782, 2006.

[2] P. S. Grant, F .Castles, Q. Lei, Y. Wang, J. M. Janurudin, D. Isakov, S. Speller, C. Dancer and C. R. M. Grovenor, *Manufacture of electrical and magnetic graded and anisotropic materials for novel manipulations of microwaves*, Philos. Trans. R. Soc. A. 373, 20140353–14, 2015.

[3] R. C. Rumpf, J. J. Pazos, J. L. Digaum, S. M. Kuebler, *Spatially variant periodic structures in electromagnetics*, Philos. Trans. R. Soc. A, 373, 20140359–22, 2015.

[4] Y. Zhang, Y. et al. Printing, folding and assembly methods for forming 3D mesostructures in advanced materials. Nat. Rev. Mater. 2, 1701917 (2017).

[5] YI, J., Piau, G.-P., de Lustrac, A. Burokur, S. N. Electromagnetic field tapering using all-dielectric gradient index materials. Sci. Rep. 17 (2016). doi:10.1038/srep30661

[6] YI, J., Burokur, S. N., Piau, G.-P. de Lustrac, A. 3D printed broadband transformation optics based all-dielectric microwave lenses. J. Opt. 18, 114 (2016).

[7] D. Isakov, C. J. Stevens, F. Castles, P. S. Grant, *3D-Printed High Dielectric Contrast Gradient Index Flat Lens for a Directive Antenna with Reduced Dimensions*, Adv. Mater. Technol. 1600072-6, 2016.

[8] Y. Wu, D. Isakov, P. S. Grant, *Fabrication of Composite Filaments with High Dielectric Permittivity for Fused Deposition 3D Printing*, Materials, (accepted) 2017.

[9] D. Isakov, Q. Lei, F. Castles, C.J. Stevens, C.R.M. Grovenor, P.S. Grant, *3D printed anisotropic dielectric composite with meta-material features*, Mat. Des., 93, 423, 2016.

[10] Q. Zhao, J. Zhou, F. Zhang, D. Lippens, *Mie resonance based dielectric metamaterials*, Mater. Today, 12, 60, 2009.

[11] D. Aspnes. *Bounds on allowed values of the effective dielectric function of two-component composites at finite frequencies*, Phys. Rev. B 25, 1358, 1982.

[12] T.D. Drysdale, B. Allen, et al., *How orbital angular momentum modes are boosting the performance of radio links*, submitted to IET Microw. Ant. Propag., 2017.

[13] Q. Lei, R. Foster, P. S. Grant, C. Grovenor, *Generalized Maxwell Fish-Eye Lens as a Beam Splitter: A Case Study in Realizing All-Dielectric Devices From Transformation Electromagnetics*, IEEE Trans. Microw. Theory, DOI: 10.1109/TMTT.2017.2727495, 2017.